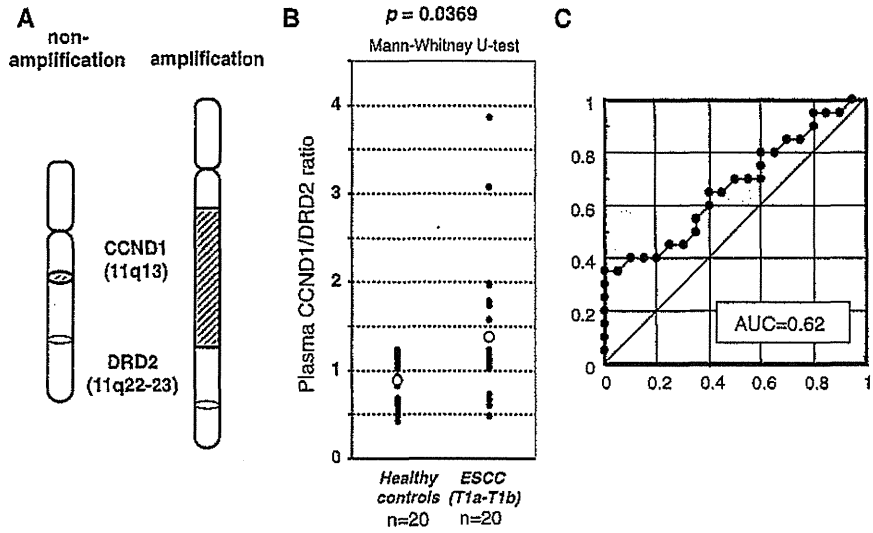

Fig. 1 **a** Measurement of the copy number in a CCND1 gene-amplified chromosome. To avoid the influences of plasma DNA quantity and numerical chromosomal aberrations, we invented and calculated the ratio of the dosage of CCND1 to that of the reference single copy gene, dopamine receptor D2 (DRD2) mapped to 11q22–23, as an indicator of the CCND1 copy number (CCND1/DRD2: C/D ratio). **b** Demonstration of the feasibility of evaluating the CCND1/DRD2 ratio in a test scale. The plasma C/D ratio was significantly higher in the superficial ESCC patient group than in the control group in the test scale ($p = 0.0369$). **c** The receiver-operating characteristic (ROC) curve for the plasma CCND1/DRD2 ratio analysis. The area under the receiver-operating characteristic curve (AUC) was 0.62

(Fig. 1a). The serum dosages of CCND1 and DRD2 were quantified by DNA based real-time PCR using the Applied Biosystems 7300 Real-Time PCR system (Applied Biosystems, Foster City, CA, USA). The final volume of the PCR mixture was 20 μl, containing 10 μl TaqMan® Universal PCR Master Mix (Applied Biosystems), 1 μl TaqMan® Copy Number Assay, and 9 μl of each DNA sample. TaqMan® Copy Number Assays for CCND1 (Hs03772544_cn) and DRD2 (Hs05266854_cn) were purchased from Applied Biosystems. All PCR reactions were performed with one cycle of 95 °C for 10 min, followed by PCR amplification with 40 cycles of 95 °C for 15 s and 60 °C for 60 s. The CCND1 copy numbers of DNA samples were determined by the ratio of the CCND1 dosage to the DRD2 dosage (C/D ratio) using the comparative threshold cycle method.

To obtain additional evidence that circulating DNA derived from tumors affects the plasma C/D ratio, postoperative plasma samples (1 month after operation) were collected from six patients in the high plasma C/D ratio group among the test scale patients who underwent curative esophagectomy. Paraffin-embedded esophageal tumor tissues and adjacent normal esophageal tissues were collected from the same six patients with high plasma C/D ratios.

Statistical Analysis

Differences in the plasma C/D ratio between the ESCC and healthy volunteer control groups were assessed using the Mann–Whitney *U* test, while those between preoperative and postoperative samples were assessed using the Wilcoxon *t* test. The chi-squared test and Fisher's exact probability test were used to evaluate correlations between the plasma C/D ratio and clinicopathological factors. *p* values less than 0.05 were considered significant. The recurrence-free survival rate was calculated using the Kaplan–Meier method, and the significance of differences was determined by the log-rank test. Multivariate stepwise logistic regression analysis was performed to identify independent risk factors associated with recurrence. Multivariate odds ratios are presented with 95 % confidence intervals.

Results

Demonstration of the Feasibility to Evaluate the CCND1/DRD2 Ratio in a Test Scale

To avoid the influences of plasma DNA quantity and chromosomal aneuploidy, we invented and calculated the ratio of the dosage of CCND1 to that of the reference single copy gene, DRD2 mapped to the same long arm of chromosome 11q22–23 as an indicator of CCND1 amplification (CCND1/DRD2: C/D ratio) (Fig. 1a) [18]. The plasma C/D ratios of 20 consecutive superficial ESCC patients and 20 healthy volunteer controls were examined to demonstrate

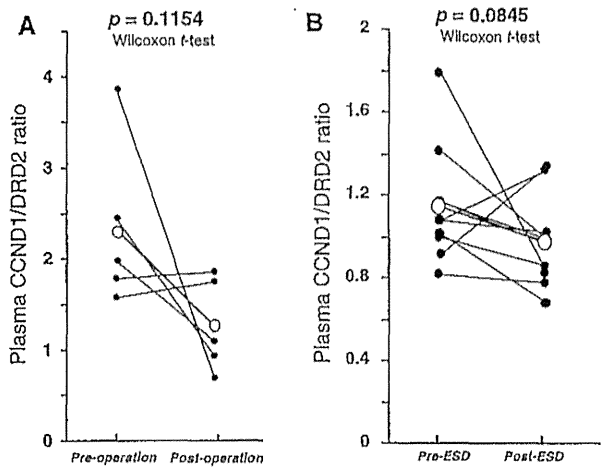

Fig. 2 Comparison of plasma CCND1/DRD2 ratios between pre-tumor resection and post-tumor resection in patients with ESCC. a The C/D ratio was slightly lower in postoperative plasma samples ($p = 0.1154$). b The C/D ratio was slightly lower in ten patients following endoscopic tumor resection ($p = 0.0845$)

the feasibility of this study. Figure 1b shows the distribution of the plasma C/D ratio in the superficial ESCC patient and control groups. The plasma C/D ratio was significantly higher in the superficial ESCC patient group than in the control group [mean ± SD: 1.38 ± 0.86 (range 0.48–3.86) vs. 0.89 ± 0.29 (0.41–1.23), $p = 0.0369$]. The area under the receiver-operating characteristic curve (AUC) was 0.62 (Fig. 1c). These results indicate that this plasma assay may ensure the feasibility of predicting the CCND1 status in superficial ESCC patients. Therefore, we performed further analyses.

Evaluation of Whether the Plasma CCND1/DRD2 Ratio Could Reflect Tumor Dynamics

We investigated whether the higher C/D ratio in the plasma could reflect the tumor status of CCND1 in superficial ESCC patients. We analyzed the C/D ratio of both esophageal cancer and adjacent normal esophageal tissues in six ESCC patients with high plasma C/D ratios. The higher C/D ratio of esophageal tumors than that of normal tissues was found in four of the six patients (67 %) (Supplementary Table 1). These results indicate that a high plasma C/D ratio reflects the CCND1 status of ESCC tumors. Moreover, we compared plasma C/D ratios between pre-tumor resection and post-tumor resection in patients with ESCC. We examined C/D ratios in the postoperative plasma samples of six patients with high plasma C/D ratios in preoperative plasma samples. The C/D ratio was slightly lower in postoperative plasma samples ($p = 0.1154$; Fig. 2a). C/D ratios were slightly lower in ten patients following endoscopic tumor resection ($p = 0.0845$) (Fig. 2b). These results suggest that the tumor CCND1 status may affect the plasma C/D ratio even in superficial ESCC patients.

Validation Study on the Clinical Application of the CCND1/DRD2 Ratio Assay Using Plasma DNA as a Diagnostic Biomarker in Superficial ESCC Patients

A total of 63 consecutive patients were included in the validation study. The mean age of these patients was 63.0 years (range 48–77), the male:female ratio was 6:1, and nine had TNM stage 0, 36 stage I, 13 stage II, one stage III, and four stage IV. All patients with stage IV had solitary distant lymph node metastasis (M1) that was curatively resected by three-field lymphadenectomy, which is mainly performed in Japan. The mean follow-up period was 24.0 months (range 1.9–63.6). The plasma C/D ratios of 63 ESCC patients and 40 healthy volunteer controls were assessed using real-time PCR to determine the cutoff value. No significant difference was observed in the plasma C/D ratio according to each stage ($p = 0.3611$, Kruskal–Wallis H test, data not shown). Figure 3a shows the distribution of the plasma C/D ratio in ESCC patient and control groups. The plasma C/D ratio was significantly higher in the ESCC patient group than in the control group [mean ± SD, 1.64 ± 1.16 (range 0.19–7.32) vs. 0.81 ± 0.39 (0.17–1.79), $p < 0.0001$]. Figure 3b shows the receiver-operating characteristic (ROC) curves for the plasma C/D ratio analysis, and the area under the curve (AUC) was 0.758. Sensitivity was 69.8 % and specificity was 80.0 % according to the ROC curves with the Youden index [21].

Determination of the Cutoff Value for the Plasma CCND1/DRD2 Ratio and Relationship Between the Plasma CCND1/DRD2 Ratio and Clinicopathological Factors

We determined a cutoff value of 1.20 for the plasma C/D ratio based on the mean value +1 SD (0.81 + 0.39) in healthy volunteer controls to distinguish high C/D ratio patients from low ratio patients. Thirty-seven patients were categorized into the high plasma C/D ratio group and 26 patients in the low plasma C/D ratio group. Correlations between the plasma C/D ratio and clinicopathological factors in 63 ESCC patients are summarized in Table 1. Patients with high plasma C/D ratios were more likely to have lymphatic invasion (high vs. low: 22 vs. 12 %) and venous invasion (high vs. low: 14 vs. 8 %), and the frequency of recurrence was significantly higher in these patients ($p = 0.0198$). No correlation was observed between the plasma C/D ratio and other clinicopathological factors in the present study.

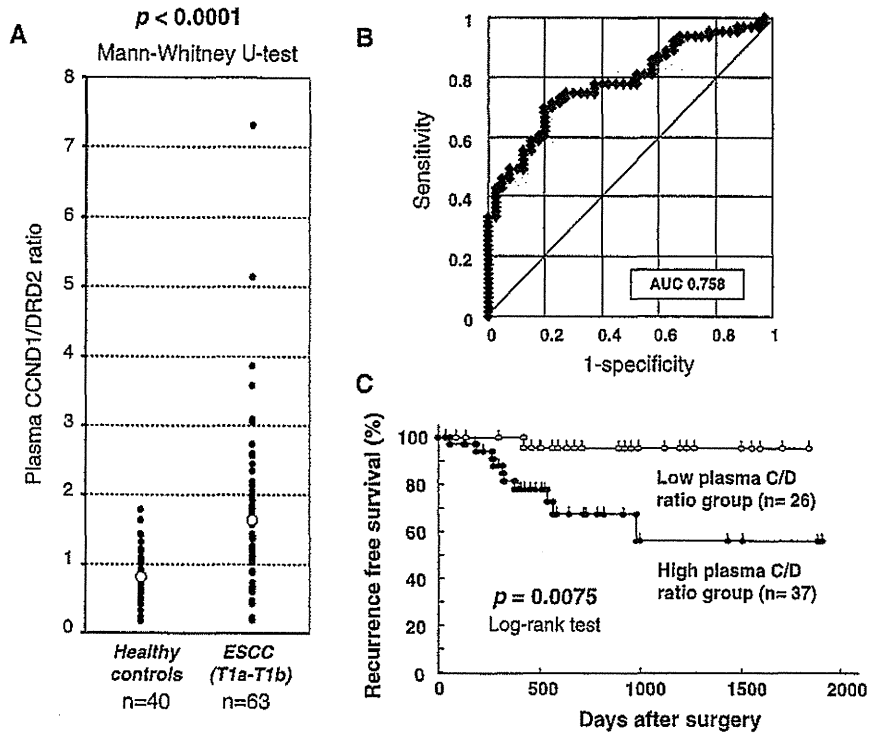

Fig. 3 Validation study on the clinical application of the plasma CCND1/DRD2 ratio assay in superficial ESCC patients. **a** The plasma C/D ratio was significantly higher in the ESCC patient group than in the control group ($p < 0.0001$). **b** The area under the curve (AUC) was 0.758. Sensitivity was 69.8 % and specificity was 80.0 % according to the ROC curves with the Younden index [21]. **c** Recurrence-free survival was significantly shorter in patients in the high plasma C/D ratio group than in those in the low ratio group ($p = 0.0075$)

Predictive Value of the Plasma CCND1/DRD2 Ratio for Recurrence in Superficial ESCC Patients

We additionally validated the predictive ability of the plasma C/D ratio for recurrence in 63 superficial ESCC patients. Recurrence-free survival was significantly shorter in patients in the high plasma C/D ratio group than in those in the low ratio group ($p = 0.0075$) (Fig. 3c). Moreover, multivariate analysis revealed the high C/D ratio to be an independent risk factor of recurrence [$p = 0.0334$; odds ratio 10.58 (range 1.203–93.23)] (Table 2).

Discussion

Gene amplification is one of the most frequent genomic aberrations involved in the pathogenesis of various cancers. Oncogenes, such as SMYD2 (1q32.3), EGFR (7p12), MYC (8q24.21), CCND1 (11q13), cIAP1 (11q22), and ERBB2 (17q21.1), have already been identified as major amplification targets associated with the development, progression, and metastasis of aggressive disease, especially in ESCC [7, 8, 18, 22–28]. CCND1, which is a key regulator of the G1 phase of the cell cycle, is the gene most frequently amplified (22–65 %) with high copy numbers and is also associated with a poorer survival outcome in ESCC patients [18, 27, 28]. CCND1 gene amplification has also been identified as a more potent prognostic factor than its

Table 1 Correlation between the plasma CCND1 amplification value and clinicopathological features

Variables	*n*	Plasma CCND1 amplification value		*p* value[a]
		Low ($n = 26$)	High ($n = 37$)	
Sex				
Male	54	25 (96 %)	29 (78 %)	
Female	9	1 (4 %)	8 (22 %)	0.0687
Age				
<65	31	15 (58 %)	16 (43 %)	
65≤	32	11 (42 %)	21 (57 %)	0.2587
Lymphatic invasion				
Negative	52	23 (88 %)	29 (78 %)	
Positive	11	3 (12 %)	8 (22 %)	0.5017
Venous invasion				
Negative	56	24 (92 %)	32 (86 %)	
Positive	7	2 (8 %)	5 (14 %)	0.6896
Lymph node metastasis				
Negative	45	20 (77 %)	25 (68 %)	
Positive	18	6 (23 %)	12 (32 %)	0.5988
Depth of invasion				
Tis-T1a	31	13 (50 %)	18 (49 %)	
T1b	32	13 (50 %)	19 (51 %)	0.9158
Recurrence				
Negative	52	25 (96 %)	27 (73 %)	
Positive	11	1 (4 %)	10 (27 %)	*0.0198*

[a] *p* values are from chi-squared or Fisher's exact test and were significant at 0.05. Values in *italic* are considered significant

Table 2 Correlation between recurrence and clinicopathological features by univariate analysis and the results of multivariable logistic regression; risk factor for recurrence

Variables	Recurrence		Univariate[a]		Multivariate[b]	
	Present ($n = 11$)	Absent ($n = 52$)	p value	OR	95 % CI	p value
Sex						
Male	10 (91 %)	44 (85 %)	1.0000			
Female	1 (9 %)	8 (15 %)			–	
Age						
<65	5 (45 %)	26 (50 %)	0.9537			
65≤	6 (55 %)	26 (50 %)			–	
Lymphatic invasion						
Negative	7 (64 %)	45 (87 %)	0.1673			
Positive	4 (36 %)	7 (13 %)			–	
Venous invasion						
Negative	9 (82 %)	47 (90 %)	0.5952			
Positive	2 (18 %)	5 (10 %)			–	
Lymph node metastasis						
Negative	5 (45 %)	40 (77 %)	0.0833			
Positive	6 (55 %)	12 (23 %)			–	
Tumor depth						
Tis-T1a	2 (18 %)	29 (56 %)		1		
T1b	9 (82 %)	23 (44 %)	*0.0398*	6.504	1.201–35.23	*0.0298*
Plasma CCND1/DRD2 ratio						
Low	1 (9 %)	25 (48 %)		1		
High	10 (91 %)	27 (52 %)	*0.0198*	10.58	1.203–93.23	*0.0334*

[a] Univariate analysis was performed using the chi-squared test and Fisher's exact probability test. Values in *italic* are considered significant

[b] Multivariable logistic regression was used to assess the risk factors for recurrence

OR odds ratio, *CI* confidence interval

CCND1 protein overexpression in cancer patients [18]. These findings prompted us to predict CCND1 amplification in the plasma samples of ESCC patients. To circumvent aneuploidy on chromosomes, we previously developed real-time quantitative PCR with a reference gene mapped to the same chromosome, and subsequently demonstrated that the ratio CCND1 (11q13)/DRD2 (11q22–23) in plasma DNA is a valuable diagnostic tool in ESCC patients [17].

Previous studies have evaluated the copy number of amplified genes in the plasma or serum [29–31]. However, few studies have used this as a therapeutic and/or diagnostic biomarker for superficial cancer or early stage cancer. Our previous studies demonstrated that the concentration of plasma DNA in cancer patients was significantly higher than that in controls, regardless of the tumor stage [20, 32]. These findings suggest that the tumor could release a significant amount of genomic DNA into the systemic circulation even at an early stage. Therefore, we hypothesized that circulating DNA in the peripheral blood may be an early event in the carcinogenesis of solid cancers, and may also allow tumor dynamics to be monitored, even at an early stage.

We investigated whether the plasma C/D ratio could reflect tumor dynamics even in superficial ESCC in the present study using three different analyses. One was a comparison between the plasma C/D ratio and CCND1 copy number in tumors, the results of which demonstrated that the tumor C/D ratio was higher than that in adjacent normal tissues in most patients with a high plasma C/D ratio. However, discrepancies were identified in some patients. One possible reason for this may have been the heterogeneity of primary tumors. Because of the genetic heterogeneity in ESCC tissue, not all ESCC show CCND1 gene amplification. Therefore, if CCND1 amplification is evaluated using several ESCC tissue samples, the rate to detect CCND1 gene amplification would increase. The second analysis involved a comparison of the plasma C/D ratio in paired plasma obtained before and after surgery. The results obtained showed that the plasma C/D ratio was slightly lower postoperatively in patients who underwent curative esophagectomy ($p = 0.1154$, Fig. 2a), which suggests that tumor-derived circulating DNA reflects the plasma C/D ratio. The third analysis was performed to demonstrate that endoscopic tumor resection also influences the plasma C/D ratio in paired plasma obtained before and after treatment. Consequently, the plasma C/D ratio was slightly lower after treatment ($p = 0.0845$, Fig. 2b). These results strongly suggest that the tumor CCND1 status may affect the plasma C/D ratio even in superficial ESCC patients. The plasma C/D ratio in some patients was slightly higher after treatment. Although this

may have been due to a margin of error, no recurrence has yet been observed in these patients. These patients will be meticulously followed up and follow-up data will be collected, especially in the plasma of patients with recurrence.

The most important result of this study was that this assay could also be used to predict recurrence in superficial ESCC. Patients with high plasma C/D ratios were more likely to have lymphatic invasion (high vs. low: 22 vs. 12 %) and venous invasion (high vs. low: 14 vs. 8 %), with the frequency of recurrence being significantly higher ($p = 0.0198$) and recurrence-free survival being significantly shorter ($p = 0.0075$). Furthermore, multivariate analysis revealed the high C/D ratio to be an independent risk factor of recurrence [$p = 0.0334$; odds ratio 10.58 (range 1.203–93.23)]. Predicting high risk patients among superficial ESCC patients after surgery and endoscopic resection is beneficial when considering additional therapies and follow-up planning.

Moreover, this assay may be more beneficial for other clinical applications in superficial ESCC because of its perspective, technical simplicity, rapidity, and reliability. In a clinical setting, gene amplification has been evaluated by fluorescence in situ hybridization (FISH), which needs several days. In contrast, this plasma assay requires only a few hours. The plasma C/D ratio assay using cell free circulating DNA, the so-called "liquid biopsy" [33], can predict the presence of CCND1 amplification in patients with micrometastasis and distant metastasis even if their ESCC tissue could not easily be obtained by tissue biopsies.

In conclusion, this noninvasive assay using circulating nucleic acids has opened up a new and interesting field in the screening and monitoring of cancer patients. We clearly demonstrated that measuring the plasma CCND1/DRD2 ratio has clinical benefits for detecting cancer and evaluating the resection status of surgery and endoscopy even in patients with superficial ESCC. We also validated its ability to predict recurrence even in superficial ESCC by analyzing the relationship between plasma results and clinicopathological factors. Our results provide evidence that the prediction of CCND1 amplification using plasma DNA could serve as a clinical biomarker for superficial ESCC.

Conflict of interest None.

References

1. Enzinger PC, Mayer RJ. Esophageal cancer. *N Engl J Med.* 2003;349:2241–2252.
2. Hiyama T, Yoshihara M, Tanaka S, Chayama K. Genetic polymorphisms and esophageal cancer risk. *Int J Cancer.* 2007;121:1643–1658.
3. Akiyama H, Tsurumaru M, Udagawa H, Kajiyama Y. Radical lymph node dissection for cancer of the thoracic esophagus. *Ann Surg.* 1994;220:364–372.
4. Noguchi H, Naomoto Y, Kondo H, et al. Evaluation of endoscopic mucosal resection for superficial esophageal carcinoma. *Surg Laparosc Endosc Percutan Tech.* 2000;10:343–350.
5. Pech O, May A, Rabenstein T, Ell C. Endoscopic resection of early oesophageal cancer. *Gut.* 2007;56:1625–1634.
6. Hollstein MC, Metcalf RA, Welsh JA, Montesano R, Harris CC. Frequent mutation of the p53 gene in human esophageal cancer. *Proc Natl Acad Sci USA.* 1990;87:9958–9961.
7. Adélaide J, Monges G, Dérdérian C, Seitz JF, Birnbaum D. Oesophageal cancer and amplification of the human cyclin D gene CCND1/PRAD1. *Br J Cancer.* 1995;71:64–68.
8. Shinozaki H, Ozawa S, Ando N, et al. Cyclin D1 amplification as a new predictive classification for squamous cell carcinoma of the esophagus, adding gene information. *Clin Cancer Res.* 1996;2:1155–1161.
9. Gratas C, Tohma Y, Barnas C, Taniere P, Hainaut P, Ohgaki H. Up-regulation of Fas (APO-1/CD95) ligand and down-regulation of Fas expression in human esophageal cancer. *Cancer Res.* 1998;58:2057–2062.
10. Kosugi S, Nishimaki T, Kanda T, Nakagawa S, Ohashi M, Hatakeyama K. Clinical significance of serum carcinoembryonic antigen, carbohydrate antigen 19-9, and squamous cell carcinoma antigen levels in esophageal cancer patients. *World J Surg.* 2004;28:680–685.
11. Mroczko B, Kozłowski M, Groblewska M, et al. The diagnostic value of the measurement of matrix metalloproteinase 9 (MMP-9), squamous cell cancer antigen (SCC) and carcinoembryonic antigen (CEA) in the sera of esophageal cancer patients. *Clin Chim Acta.* 2008;389:61–66.
12. Sozzi G, Conte D, Leon M, et al. Quantification of free circulating DNA as a diagnostic marker in lung cancer. *J Clin Oncol.* 2003;21:3902–3908.
13. Kimura H, Kasahara K, Kawaishi M, et al. Detection of epidermal growth factor receptor mutations in serum as a predictor of the response to gefitinib in patients with non-small-cell lung cancer. *Clin Cancer Res.* 2006;12:3915–3921.
14. Skvortsova TE, Rykova EY, Tamkovich SN, et al. Cell-free and cell-bound circulating DNA in breast tumours: DNA quantification and analysis of tumour-related gene methylation. *Br J Cancer.* 2006;94:1492–1495.
15. Diehl F, Schmidt K, Choti MA, et al. Circulating mutant DNA to assess tumor dynamics. *Nat Med.* 2008;14:985–990.
16. Schwarzenbach H, Alix-Panabières C, Müller I, et al. Cell-free tumor DNA in blood plasma as a marker for circulating tumor cells in prostate cancer. *Clin Cancer Res.* 2009;15:1032–1038.
17. Takeshita H, Ichikawa D, Komatsu S, et al. Prediction of CCND1 amplification using plasma DNA as a prognostic marker in oesophageal squamous cell carcinoma. *Br J Cancer.* 2010;102:1378–1383.
18. Kyomoto R, Kumazawa H, Toda Y, et al. Cyclin-D1-gene amplification is a more potent prognostic factor than its protein over-expression in human head-and-neck squamous-cell carcinoma. *Int J Cancer.* 1997;74:576–581.
19. Sobin LH, Gospodarowicz MK, Wittekind C. *TNM classification of malignant tumours.* 7th ed. Oxford: International Union Against Cancer. Wiley-Blackwell; 2009:66–72.
20. Tomita H, Ichikawa D, Ikoma D, et al. Quantification of circulating plasma DNA fragments as tumor markers in patients with esophageal cancer. *Anticancer Res.* 2007;27:2737–2741.
21. Akobeng AK. Understanding diagnostic tests 3: receiver operating characteristic curves. *Acta Paediatr.* 2007;96:644–647.
22. Komatsu S, Imoto I, Tsuda H, et al. Overexpression of SMYD2 relates to tumor cell proliferation and malignant outcome of esophageal squamous cell carcinoma. *Carcinogenesis.* 2009;30:1139–1146.
23. Kitagawa Y, Ueda M, Ando N, Ozawa S, Shimizu N, Kitajima M. Further evidence for prognostic significance of epidermal growth

factor receptor gene amplification in patients with esophageal squamous cell carcinoma. *Clin Cancer Res.* 1996;2:909–914.
24. Lu SH, Hsieh LL, Luo FC, Weinstein IB. Amplification of the EGF receptor and c-myc genes in human esophageal cancers. *Int J Cancer.* 1988;42:502–505.
25. Imoto I, Yang ZQ, Pimkhaokham A, et al. Identification of cIAP1 as a candidate target gene within an amplicon at 11q22 in esophageal squamous cell carcinomas. *Cancer Res.* 2001;61:6629–6634.
26. Mimura K, Kono K, Hanawa M, et al. Frequencies of HER-2/neu expression and gene amplification in patients with oesophageal squamous cell carcinoma. *Br J Cancer.* 2005;92:1253–1260.
27. Jiang W, Kahn SM, Tomita N, Zhang YJ, Lu SH, Weinstein IB. Amplification and expression of the human cyclin D gene in esophageal cancer. *Cancer Res.* 1992;52:2980–2983.
28. Lam AK. Molecular biology of esophageal squamous cell carcinoma. *Crit Rev Oncol Hematol.* 2000;33:71–90.
29. Chiang PW, Beer DG, Wei WL, Orringer MB, Kurnit DM. Detection of erbB-2 amplifications in tumors and sera from esophageal carcinoma patients. *Clin Cancer Res.* 1999;5:1381–1386.
30. Gotoh T, Hosoi H, Iehara T, et al. Prediction of MYCN amplification in neuroblastoma using serum DNA and real-time quantitative polymerase chain reaction. *J Clin Oncol.* 2005;23:5205–5210.
31. Park KU, Lee HE, Park DJ, et al. MYC quantitation in cell-free plasma DNA by real-time PCR for gastric cancer diagnosis. *Clin Chem Lab Med.* 2009;47:530–536.
32. Sai S, Ichikawa D, Tomita H, et al. Quantification of plasma cell-free DNA in patients with gastric cancer. *Anticancer Res.* 2007;27:2747–2751.
33. Diaz LA Jr, Williams RT, Wu J, Kinde I, et al. The molecular evolution of acquired resistance to targeted EGFR blockade in colorectal cancers. *Nature.* 2012;486:537–540.

J Gastroenterol (2014) 49:655–666
DOI 10.1007/s00535-013-0827-9

The Japanese Society of Gastroenterology

ORIGINAL ARTICLE—ALIMENTARY TRACT

The expression and role of Aquaporin 5 in esophageal squamous cell carcinoma

Hiroki Shimizu · Atsushi Shiozaki · Daisuke Ichikawa · Hitoshi Fujiwara · Hirotaka Konishi · Hiromichi Ishii · Shuhei Komatsu · Takeshi Kubota · Kazuma Okamoto · Mitsuo Kishimoto · Eigo Otsuji

Received: 29 October 2012 / Accepted: 20 April 2013 / Published online: 9 May 2013

Abstract
Background Aquaporins (AQPs) are water channel proteins that facilitate transcellular water movements. Recent studies have shown that AQP5 is expressed in various cancers, and plays a role in tumor progression. However, its expression and role in esophageal squamous cell carcinoma (ESCC) have not been investigated. We examined the pathophysiologic role of AQP5 in cell proliferation and survival, and also investigated its expression and effects on the prognosis of ESCC patients.
Methods AQP5 expression in human ESCC cell lines was analyzed by Western blot testing. Knockdown experiments with AQP5 siRNA were conducted, and the effects on cell proliferation, cell cycle progression, and cell survival were analyzed. The cells' gene expression profiles were analyzed by microarray analysis. Immunohistochemistry of AQP5 for 68 primary tumor samples obtained from ESCC patients undergoing esophagectomy was performed.
Results AQP5 expression was high in TE2 and TE5 cells. In these cells, the knockdown of AQP5 using siRNA inhibited cell proliferation and G_1-S phase progression, and induced apoptosis. The AQP5 siRNA transfected TE5 cells showed significant increase in p21 and decrease in CCND1 mRNA expression, respectively. The expression pattern of AQP5 and p21 protein was sharply contrasted, but AQP5 and CCND1 protein expression showed a similar pattern in ESCC tissue. These findings agree with the microarray results. Immunohistochemical staining of 68 ESCC patients showed the AQP5 expression is associated with tumor size, histological type, and tumor recurrence.
Conclusion The AQP5 expression in ESCC cells may affect cell proliferation and survival, and impact on the prognosis of ESCC patients.

Keywords Aquaporin 5 · Esophageal cancer · Cell proliferation

H. Shimizu and A. Shiozaki contributed equally to this work.

Electronic supplementary material The online version of this article (doi:10.1007/s00535-013-0827-9) contains supplementary material, which is available to authorized users.

H. Shimizu · A. Shiozaki (✉) · D. Ichikawa · H. Fujiwara · H. Konishi · H. Ishii · S. Komatsu · T. Kubota · K. Okamoto · E. Otsuji
Division of Digestive Surgery, Department of Surgery, Kyoto Prefectural University of Medicine, 465 Kajii-cho, Kawaramachihirokoji, Kamigyo-ku, Kyoto 602-8566, Japan
e-mail: shiozaki@koto.kpu-m.ac.jp

M. Kishimoto
Department of Pathology, Kyoto Prefectural University of Medicine, 465 Kajii-cho, Kawaramachihirokoji, Kamigyo-ku, Kyoto, Japan

Introduction

Aquaporins (AQPs) are transmembrane proteins that facilitate the movement of water across cellular membranes, and therefore play a major role in body water homeostasis [1, 2]. In addition, as membrane proteins, AQPs transport other molecules, such as urea and glycerol [3], and mediate intercellular signals [4–6]. To date, 13 AQP subtypes and their pathophysiologic roles have been characterized in humans [7, 8]. For example, AQP5 is expressed in various tissues, including salivary [9–11] and airway submucosal glands [12], pancreatic [13] and corneal epithelium [14], type I pneumocytes [15], and the kidney [16].

Recent studies have revealed that AQPs are ectopically expressed in various cancers. For instance, AQP5

is expressed in colorectal [17, 18], pancreatic [13], breast [19], lung [20–23], gastric [24], and ovarian cancers [25], and in chronic myelogenous leukemia [26]. Kang et al. [18] showed an association between the expression of AQP5 in both resected colorectal cancer tissue samples and in liver metastases. Recent molecular and biochemical studies have also shown a role for the AQPs in human carcinogenesis. Zhang et al. [23] showed that AQP5 promotes cell proliferation and migration in lung cancer. According to Kusayama et al. [27], AQP3 is expressed and plays a role in esophageal squamous cell carcinoma (ESCC); however, the expression and pathophysiologic role of AQP5 in human ESCC is unknown.

The objective of the present study was to investigate how AQP5 may regulate genes involved in cell cycle progression and cell death and the clinicopathological significance of AQP5 expression in ESCC. A microarray analysis showed that transfection with AQP5 siRNA changed the expression level of many genes related to tumor growth and apoptosis. Further, AQP5 expression in human ESCC samples was associated with clinicopathological features and prognosis, establishing an important role for AQP5 in ESCC tumor progression.

Materials and methods

Cell lines, antibodies, and other reagents

Poorly differentiated human ESCC cell lines, TE2, TE5, TE9, and TE13, were obtained from the Cell Resource Center of Biomedical Research Institute of Development, Aging, and Cancer (Tohoku University, Sendai, Japan) [28]. Poorly differentiated human ESCC cell line, KYSE70, and moderately differentiated human ESCC cell line, KYSE170, were obtained from Kyoto University (Kyoto, Japan) [29]. The cells were maintained in RPMI 1640 medium (Nacalai Tesque, Kyoto, Japan) with 10 % fetal bovine serum (FBS) and 1 % penicillin–streptomycin and were cultured in a standard humidified incubator at 37 °C with 5 % CO_2.

The following antibodies were used in the study; (1) a monoclonal AQP5 antibody (Abcam, Cambridge, MA, UK), (2) a polyclonal p21 antibody (Cell Signaling Technology, Beverly, MA, USA), (3) a monoclonal cyclin D1 (CCND1) antibody (clone SP4, Abcam, Cambridge, MA, UK), (4) a horseradish peroxidase (HRP)-conjugated anti-rabbit secondary antibody (Cell Signaling Technology, Beverly, MA), and (5) a glyceraldehyde-3-phosphate dehydrogenase (GAPDH) antibody (Santa Cruz Biotechnology, Santa Cruz, CA, USA).

Protein studies

Cells were harvested in M-PER lysis buffer supplemented with protease inhibitors (Pierce, Rockford, IL, USA). The protein concentration was measured with a modified Bradford assay (Bio-Rad, Hercules, CA, USA). Cell lysates containing equal amounts of total protein were separated by SDS-PAGE and then were transferred onto PVDF membranes (GE Healthcare, Piscataway, NJ, USA). The membranes were probed with the indicated antibodies, and proteins were detected by the ECL Plus Western Blotting Detection System (GE Healthcare).

Small interfering RNA (siRNA) transfection

Cells were transfected with 10 nmol/L AQP5 siRNA (Stealth RNAi™ siRNA #HSS100611; Invitrogen, Carlsbad, CA, USA) using the Lipofectamine RNAiMAX reagent (Invitrogen) according to the manufacturer's instructions. The medium containing the siRNA was replaced with fresh medium after 24 h. The provided control siRNA (Stealth RNAi™ siRNA Negative Control; Invitrogen) was used as a negative control.

Real-time quantitative RT-PCR

Total RNA was extracted using an RNeasy kit (Qiagen, Valencia, CA, USA). Messenger RNA (mRNA) expression was measured by a quantitative real-time PCR (7300 Real-Time PCR System; Applied Biosystems, Foster City, CA) using TaqMan Gene Expression Assays (Applied Biosystems) according to the manufacturer's instruction. Expression levels were measured for the following genes: AQP5 (Hs00387048_m1), CELF2 (Hs00272516_m1), CCND1 (Hs00765553_m1), TP53INP1 (Hs01003820_m1), CDKN1A (p21) (Hs00355782_m1), CXCR7 (Hs00664172_s1), and SERPINB9 (Hs00394497_m1) (Applied Biosystems). For each gene, expression was normalized against the housekeeping gene beta-actin (ACTB, Hs01060665_g1; Applied Biosystems). Each assay was performed in triplicate.

Cell cycle analysis

The cell cycle progression was evaluated at 48 h after the siRNA transfection by fluorescence-activated cell scoring (FACS). Briefly, the cells were treated with Triton X-100 and RNase, and their nuclei were stained with propidium iodide (PI). DNA content was then measured using a Becton–Dickinson FACS Calibur (Becton–Dickinson, Mountain view, CA, USA). At least 10,000 cells were counted, and ModFit LT software (Verity Software House,

Topsham, ME, USA) was used to analyze cell cycle distribution.

Cell proliferation

Cells were seeded onto six-well plates at a density of 1.0×10^5 cells per well and incubated at 37 °C with 5 % CO_2. At 24 h after the cell seeding, siRNA transfection was performed. At 48 h after siRNA transfection, the cells were detached from the flasks using a trypsin–EDTA solution and were counted with a hemocytometer.

Analysis of apoptotic cells

Cells were treated with staurosporine, which induced intrinsic apoptosis via activation of caspase-3, for 24 h. Then, cells were harvested and stained with fluorescein isothiocyanate-conjugated annexin V and phosphatidylinositol using the annexin V kit (Beckman Coulter, Brea, CA, USA) according to the manufacturer's protocols. A Becton–Dickinson FACS Calibur was used to analyze the proportion of apoptotic cells.

Patients and primary tissue samples

Histologically proven primary ESCC tumor samples were obtained from 68 consecutive patients with who underwent esophagectomy (potentially curative R0 resection) at Kyoto Prefectural University of Medicine (Kyoto, Japan) between 1998 and 2009. Tumor samples were embedded in paraffin after 12 h formalin fixation. The patient eligibility criteria were as follows: (1) the presence of ESCC, (2) the absence of synchronous or metachronous cancers, (3) a lack of preoperative radiation therapy. All patients gave written informed consent. Relevant clinicopathological and survival data were obtained from the hospital records. Cancer recurrence occurred in 28 patients (41.2 %) during the follow-up period. The initial recurrence pattern detected by imaging studies was classified as locoregional, distant, or both sites. Twenty-two patients (32.4 %) died of cancer recurrence, and 1 patient (1.5 %) died of other disease. The median follow-up period of all patients was 45.2 months (range, 4–157 months). Staging was primarily based on the International Union Against Cancer (UICC)/TNM Classification of Malignant Tumors (7th edition) [30].

Immunohistochemistry

Paraffin sections (4 μm in thickness) of the tumor tissues were subjected to immunohistochemical staining for the AQP5 protein using the Avidin–biotin-peroxidase complex method. Briefly, paraffin sections were dewaxed in xylene and dehydrated through a graded series of alcohols. Antigen retrieval was performed by heating the samples in Dako REAL Target Retrieval Solution (Glostrup, Denmark) for 40 min at 98 °C. Endogenous peroxidases were quenched by incubating the sections for 30 min in 0.3 % H_2O_2. The sections were then treated with protein blocker and incubated overnight at 4 °C with anti- AQP5 (1 :100), p21 (1 : 1000), and CCND1 (1 : 100) antibody diluted in PBS. The avidin–biotin-peroxidase complex system (Vectastain ABC Elite kit; Vector laboratories, Burlingame, CA, USA) was used with diaminobenzidine tetrahydrochloride for color development. The sections were counterstained with hematoxylin. Finally, the sections were dehydrated through a graded series of alcohols, cleared in xylene, and mounted.

AQP5 expression levels of immunohistochemically stained samples were graded semiquantitatively, considering both the staining intensity and the percentage of positive tumor cells. The staining intensity was scored as either 0 (no reactive), 1 (weakly reactive), 2 (moderately reactive), or 3 (strongly reactive). The proportion of positive tumor cells was scored as 0 (0–10 %), 1 (11–30 %), 1.5 (31–50 %), or 2 (51 % or more). Each sample's score was determined as the maximum multiplied product of the intensity and proportion scores [18, 31, 32]. Scores of 3 or more and scores less than 3 were defined as AQP5 expression positive and AQP5 expression negative, respectively.

Microarray sample preparation and hybridization

TE5 cells were transfected with control siRNA and AQP5 siRNA ($n = 1$). At 48 h after siRNA transfection, total RNA was extracted using an RNeasy kit (Qiagen). RNA quality was monitored using an Agilent 2100 Bioanalyzer (Agilent Technologies, Santa Clara, CA). Cyanine-3 (Cy3)-labeled cRNA was prepared from 0.1 μg Total RNA using the Low Input Quick Amp Labeling Kit (Agilent) according to the manufacturer's instructions. Samples were purified using RNAeasy columns (Qiagen). A total of 0.60 μg of Cy3-labelled cRNA was fragmented and hybridized to an Agilent SurePrint G3 Human Gene Expression 8 × 60 K Microarray for 17 h. After washing, slides were scanned immediately on the Agilent DNA Microarray Scanner (G2565CA) using the one-color scan setting for 8 × 60 K array slides.

Processing of microarray data

The scanned images were analyzed with Feature Extraction Software 10.10 (Agilent) using default parameters to obtain background subtracted and spatially detrended processed signal intensities. The fold change of each molecule was

calculated by using raw signal data of two samples, and a fold change cutoff of 2 was set to identify molecules whose expression was significantly differentially regulated. The networks and functional analyses were generated through the use of Ingenuity Pathway Analysis (IPA) (Ingenuity Systems, Inc., Redwood City, CA). A network is a graphical representation of the molecular relationships between molecules. Molecules are represented as nodes, and the biological relationship between two nodes is represented as an edge. The functional analysis identified the biological function and/or diseases that were most significant to the data set.

Statistical analysis

Chi-square or Fisher's exact tests were used to evaluate differences between proportions, and Student's t test was used to evaluate continuous variables. Survival curves were constructed by the Kaplan–Meier method, and differences in survival were examined using the log-rank test. Cox proportional hazard model was used to identify prognostic factors. Differences were considered significant when the relevant p value was <0.05. These analyses were performed using the JMP statistical software package (JMP, version 10, SAS Institute Inc., Cary, NC, USA).

Results

Expression of Aquaporin 5 in ESCC cells

To determine the role of AQP5 in ESCC, we first examined six ESCC cell lines, TE2, TE5, TE9, TE13, KYSE70, and KYSE170, for AQP5 protein expression. Western blotting of these cell lines showed that AQP5 expression was high in TE2 and TE5 cells, low in TE13 cells, and nearly absent in TE9, KYSE70, and KYSE170 cells (Fig. 1). Further, there was no correlation between AQP5 protein expression and histological differentiation (Supplementary Fig. 1).

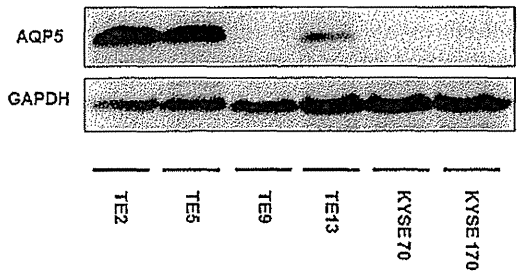

Fig. 1 Expression of Aquaporin 5 in ESCC cells. AQP5 protein expression was analyzed in 6 ESCC cell lines. Western blotting showed that AQP5 expression was high in TE2 and TE5 cells, low in TE13 cells, and nearly absent in TE9, KYSE70, and KYSE170 cells

Aquaporin 5 controls cell cycle progression in ESCC cells

We conducted knockdown experiments with AQP5 siRNA in TE2 and TE5 cells to analyze effects on cell cycle progression. In both cell lines, AQP5 siRNA effectively reduced both AQP5 protein (Fig. 2a) and mRNA (Fig. 2b). The down-regulation of AQP5 partially reduced cell cycle progression from the G_1 to S phase (Fig. 2c). At 48 h after siRNA transfection, cell counts were significantly lower in AQP5 siRNA transfected cells relative to the control (Fig. 2d). These results suggest that AQP5 plays an important role in the regulation of cell cycle progression and cell proliferation in ESCC cells.

Further, we showed no significant difference in cell proliferation between AQP5 and control siRNA transfected conditions in TE9 and KYSE70 cells, in which AQP5 expression was nearly absent (Supplementary Fig. 2). We also performed knockdown experiment with another AQP5 siRNA (AQP5 siRNA #2, Stealth RNAi™ siRNA #HSS179941) in TE5 cells, and showed the similar results in cell cycle and cell proliferation as described in Fig. 2 (Supplementary Fig. 2).

Aquaporin 5 controls the survival of ESCC cells

To determine the role of AQP5 in ESCC cell survival, we treated TE2 and TE5 cells with AQP5 siRNA and analyzed apoptosis. Down-regulation of AQP5 induced early apoptosis (annexin V positive/PI negative) in TE5 cells and late apoptosis (annexin V/PI double positive) in TE2 and TE5 cells 48 h after siRNA transfection (Fig. 3). Further, AQP5 siRNA enhanced staurosporine (200 nmol/L) stimulus-induced late apoptosis in TE2 and TE5 cells (Fig. 3). These findings indicate that AQP5 expression influences cell survival in TE2 and TE5 cells.

Gene expression profiling in Aquaporin 5 siRNA transfected cells

To determine the molecular mechanisms by which AQP5 regulates cellular functions, we determined the microarray gene expression profiles of AQP5 siRNA transfected TE5 cells and control siRNA transfected TE5 cells and analyzed the results using bioinformatic approaches. The microarray analysis showed 2,132 genes with fold changes of $\geqq 2$ in TE5 cells subjected to AQP5 knockdown. Of these genes, 1,472 were up-regulated, and 660 were down-regulated. The 20 genes whose expression was most strongly up- or down-regulated are shown in Table 1. IPA showed that the top-ranked network related to AQP5 knockdown was "Cellular Growth and Proliferation" (Supplementary Table 1). Among the 2132 genes with altered expression in

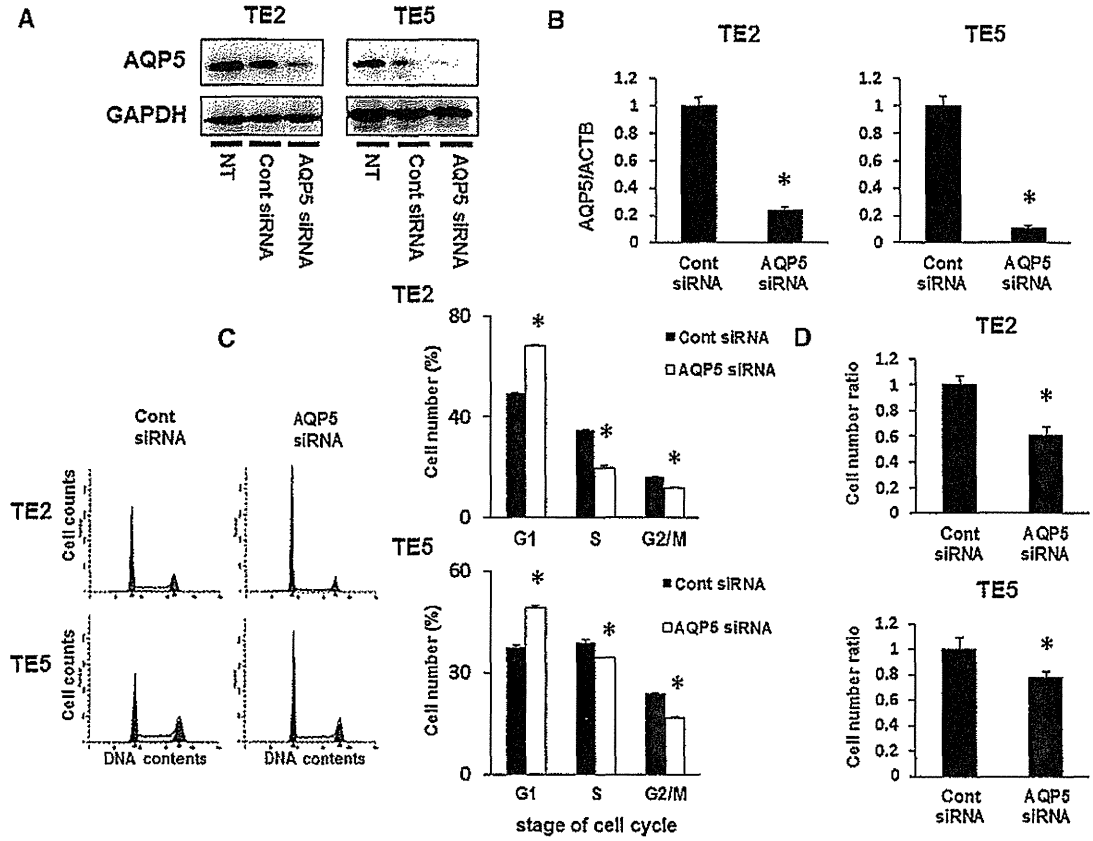

Fig. 2 Aquaporin 5 controls the cell cycle progression of ESCC cells. a Western blotting revealed that AQP5 siRNA effectively reduced the AQP5 protein in TE2 and TE5 cells. b AQP5 siRNA effectively reduced the AQP5 mRNA in TE2 and TE5 cells. Mean ± SEM. $n = 3$. $^*p < 0.05$ (compared with control siRNA). c AQP5 down-regulation partially reduced cell cycle progression from G_1 to S phase in TE2 and TE5 cells. Cells transfected with control or AQP5 siRNA were stained with propidium iodide (PI) and analyzed by flow cytometry. Mean ± SEM. $n = 3$. $^*p < 0.05$ (compared with control siRNA). d AQP5 down-regulation inhibited the proliferation of TE2 and TE5 cells. The number of cells was counted at 48 h after siRNA transfection. Mean ± SEM. $n = 3$. $^*p < 0.05$ (compared with control siRNA)

the AQP5 knockdown cells, 398 genes had cell proliferation-related functions (cellular growth and proliferation, 223 genes; cell cycle, 68 genes; cell death, 176 genes; or cellular development, 234 genes) (Supplementary Table 2). Of these genes, 277 genes were upregulated and 121 genes were downregulated (Supplementary Table 2). We then specifically examined the signal transduction networks induced by the knockdown AQP5. The top-ranked signaling network was "Cellular development, Cellular growth and proliferation, Renal proliferation" (Supplementary Fig. 3). These results indicate that AQP5 expression influences cellular growth and proliferation genes.

Verification of gene expression by real-time quantitative RT-PCR

To confirm the results of microarray analysis, we selected six genes (CELF2, CXCR7, SERPINB9, TP53INP1, CCND1, CDKN1A). CELF2 was one of the top ranked downregulated genes (Table 1), and contained in the top-ranked signaling network (Supplementary Fig. 3). CXCR7 and SERPINB9 were ones of the top ranked upregulated genes (Table 1), and included in cell growth or survival-related genes (Supplementary Table 2). TP53INP1, p53 inducible nuclear protein 1, was also one of the top ranked up-regulated genes (Table 1), and p53 was widely known as the gene related to cell apoptosis. CCND1 and CDKN1A were included in significantly changed genes (Supplementary Table 2), and well known G1 to S phase transition related genes. The expression of the six genes was examined using quantitative RT-PCR. For each gene, expression levels were compared between the AQP5 siRNA transfected TE5 cells and the control siRNA transfected TE5 cells. Relative to the control, the AQP5 siRNA transfected TE5 cells showed significantly decreased mRNA expression for the CELF2 and CCND1 genes and a significant increase in mRNA expression for the TP53INP1, CDKN1A, CXCR7, and SERPINB9 genes (Fig. 4). These changes agree with the microarray results.

We also examined and compared the expression levels of these six genes in three nontreated cell lines, TE5 (with high

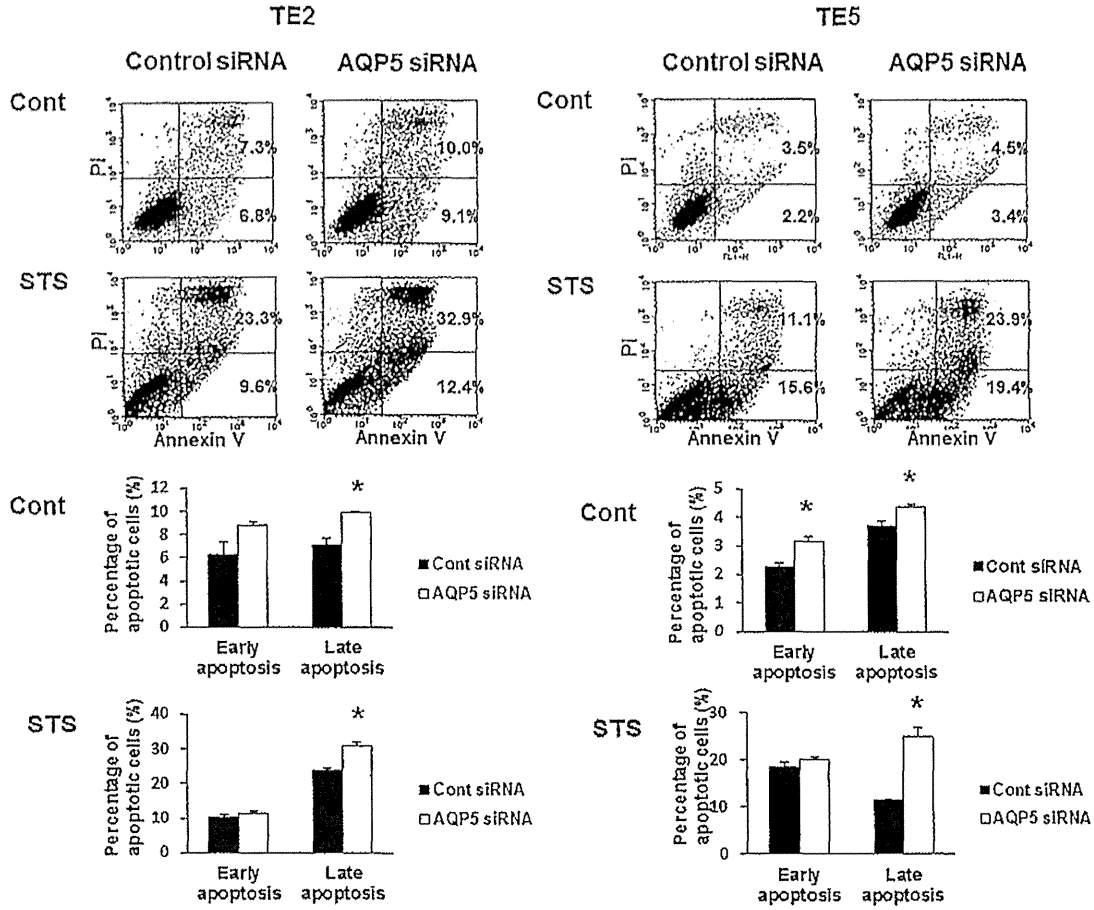

Fig. 3 Aquaporin 5 controls the survival of ESCC cells. AQP5 down-regulation enhanced spontaneous and induced cell death in TE2 and TE5 cells. Cells transfected with control or AQP5 siRNA were treated with staurosporine (200 nmol/L) for 24 h. Mean ± SEM. $n = 3$. $^*p < 0.05$ (compared with control siRNA)

expression of AQP5), TE13 (with moderate expression of AQP5), and TE9 (with low expression of AQP5). However, there was no correlation between the expression levels of AQP5 and the six genes as shown in Fig. 4 (Supplementary Fig. 4). These results indicated that the genetic background of these genes was variant between cell lines.

Aquaporin 5 protein expression in human ESCC

We further examined the expression of AQP5 in 68 primary tumor samples of human ESCC based on their immunohistochemical reactivity. The AQP5 protein was expressed in cytoplasm of the carcinoma cells (Fig. 5a). Figure 5b shows panels of the four immunohistochemical staining intensity scores for AQP5. In all of the samples, the AQP5 protein was not expressed in noncancerous esophageal epithelia (Supplementary Fig. 5A). On the other hand, the AQP5 protein was found in the early stage of ESCC, intramucosal carcinoma (Supplementary Fig. 5B). The immunohistochemical staining patterns of AQP5, p21, and CCND1 protein supported the results of microarray and verification studies as described in Supplementary Table 2 and Fig. 4. In details, the expression pattern of AQP5 and p21 protein was sharply contrasted, but on the other hand, AQP5 and CCND1 protein expression showed a similar pattern (Fig. 6).

We compared two groups that were established based on the AQP5 staining scores described in the "Methods" section. Of the 68 patients, 27 (40 %) were AQP5 negative, and 41 (60 %) were AQP5 positive. Tumor size and histological type were significantly associated with AQP5 expression (Table 2). However, AQP5 expression was not correlated with other clinicopathological variables, including gender, age, presence of preoperative chemotherapy, lymphatic invasion, venous invasion, pathological depth of tumor, lymph node metastasis and stage, or presence of postoperative recurrence within 3 years (Table 2). We also assessed whether AQP5 expression was prognostic for ESCC patients after curative resection. The 3-year progression-free survival (PFS) rate of the AQP5 positive group was 53.7 %, which was significantly poorer than that of the AQP5 negative group (77.8 %) ($p = 0.045$)

Table 1 The 20 genes that displayed the greatest changes in their expressions in the Aquaporin 5 siRNA transfected TE5 cells

Gene symbol	Gene ID	Gene name	Fold change
Up-regulated genes			
GCET2	NM_001190259	Germinal center expressed transcript 2	25.47
SERPINB9	NM_004155	Serpin peptidase inhibitor, clade B (ovalbumin), member 9	18.88
SVOP	NM_018711	SV2 related protein homolog (rat)	15.06
CXCR7	NM_020311	Chemokine (C-X-C motif) receptor 7	13.75
PTX3	NM_002852	Pentraxin 3, long	13.47
PLCB1	NM_182734	Phospholipase C, beta 1 (phosphoinositide-specific)	13.29
RAD21L1	NM_001136566	RAD21-like 1 (*S. pombe*)	12.18
EYA4	NM_004100	Eyes absent homolog 4 (Drosophila)	12.12
CLEC2D	NM_013269	C-type lectin domain family 2, member D	11.63
PCDHB9	NM_019119	Protocadherin beta 9	11.08
PGM2L1	NM_173582	Phosphoglucomutase 2-like 1	11.08
LYPD4	NM_173506	LY6/PLAUR domain containing 4	10.88
RBFOX1	NM_145893	RNA binding protein, fox-1 homolog (*C. elegans*) 1	10.84
LSS	NM_001001438	Lanosterol synthase (2,3-oxidosqualene-lanosterol cyclase)	10.43
ACTG2	NM_001615	Actin, gamma 2, smooth muscle, enteric	10.12
TP53INP1	NM_033285	Tumor protein p53 inducible nuclear protein 1	10.08
P2RY6	NM_176798	Pyrimidinergic receptor P2Y, G-protein coupled, 6	9.32
ITPR1	NM_002222	Inositol 1,4,5-trisphosphate receptor, type 1	9.11
FEZF2	NM_018008	FEZ family zinc finger 2	9.10
ENKUR	NM_145010	Enkurin, TRPC channel interacting protein	8.78
Down-regulated genes			
CSRP1	AK126507	Cysteine and glycine-rich protein 1	−124.09
ABCA8	NM_007168	ATP-binding cassette, sub-family A (ABC1), member 8	−68.69
TRPM6	NM_017662	Transient receptor potential cation channel, subfamily M, member 6	−53.54
GHR	NM_001242462	Growth hormone receptor	−30.83
GPR34	NM_001097579	G protein-coupled receptor 34	−28.26
ASGR1	NM_001671	Asialoglycoprotein receptor 1	−26.45
CELF2	NM_001025077	CUGBP, Elav-like family member 2	−23.91
APOC3	NM_000040	Apolipoprotein C-III	−23.60
OMG	NM_002544	Oligodendrocyte myelin glycoprotein	−23.15
GAS7	NM_201433	Growth arrest-specific 7	−23.06
ARHGAP24	NM_001025616	Rho GTPase activating protein 24	−23.00
CD72	NM_001782	CD72 molecule	−21.88
MPP4	NM_033066	Membrane protein, palmitoylated 4 (MAGUK p55 subfamily member 4)	−21.39
MYO7A	NM_000260	Myosin VIIA	−19.63
PLEKHG1	NM_001029884	Pleckstrin homology domain containing, family G (with RhoGef domain) member 1	−18.41
NTNG1	NM_001113228	Netrin G1	−18.34
FRMPD2	NM_001018071	FERM and PDZ domain containing 2	−18.03
DLC1	NM_024767	Deleted in liver cancer 1	−17.49
CHST10	NM_004854	Carbohydrate sulfotransferase 10	−16.09
GJA1	NM_000165	Gap junction protein, alpha 1, 43 kDa	−16.06

(Fig. 7a). The univariate analysis showed that the presence of lymphatic invasion, venous invasion, and lymph node metastasis were also correlated with a poor 3-year PFS rate. The multivariate analysis with these four factors revealed that the presence of lymph node metastasis was the only independent prognostic factor (Table 3). Regarding the pattern of postoperative recurrence within 3 years, the number of patients with an initial recurrence at locoregional, distant, and both sites were 1, 3, and 2 in the AQP5 negative group, and 7, 10, and 2 in the AQP5 positive group, respectively, and there was no significant difference between two groups ($p = 0.748$) (Supplementary Table 3).

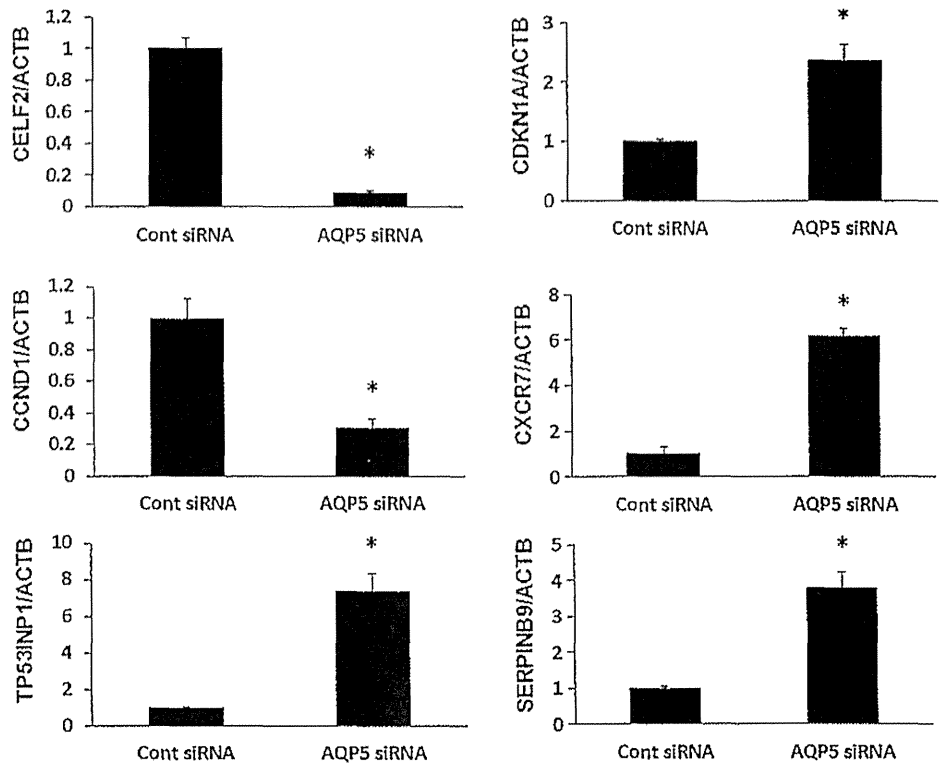

Fig. 4 Verification of gene expression by real-time quantitative RT-PCR. The expression of six selected genes (CELF2, CCND1, TP53INP1, CDKN1A, CXCR7, SERPINB9) in AQP5 siRNA transfected TE5 cells were compared with those in control siRNA transfected cells using real-time quantitative RT-PCR. Expression of each gene was normalized against ACTB. Mean ± SEM. $n = 3$. *$p < 0.05$ (compared with control siRNA)

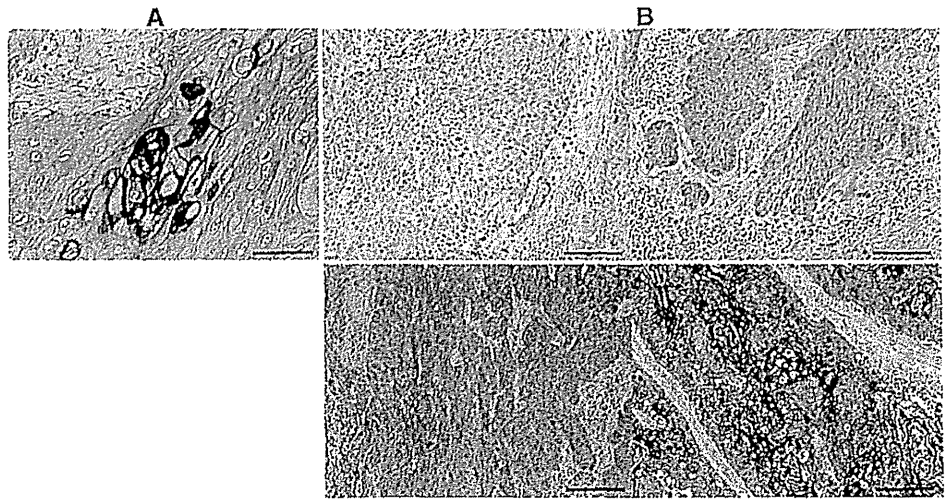

Fig. 5 Aquaporin 5 protein expression in human ESCC tissues. a Immunohistochemical staining of human ESCC samples with AQP5 antibody revealed that the AQP5 protein was expressed in cytoplasm of the carcinoma cells. Magnification: ×400. *Bar* 100 μm. b Photomicrographs of AQP5 immunohistochemistry are shown with the examples of score 0 (*upper left*), score 1 (*upper right*), score 2 (*lower left*), and score 3 (*lower right*). Magnification: ×200. *Bar* 200 μm

The 3-year overall survival rate of the AQP5 positive group, however, was 65.9 % and poorer than that of the AQP5 negative group (81.5 %). No significant difference was detected between two groups ($p = 0.160$) (Fig. 7b).

These findings suggest that AQP5 expression is induced in ESCC, and higher AQP5 expression might be related to the prognosis of patients with ESCC after curative resection.

Discussion

This is the first study to report both on the expression of AQP5 in human ESCC tissue and on the pathophysiologic role of AQP5 expression in ESCC cells. The aquaporins represent a family of transmembrane water channel proteins that are widely expressed across tissues and play a

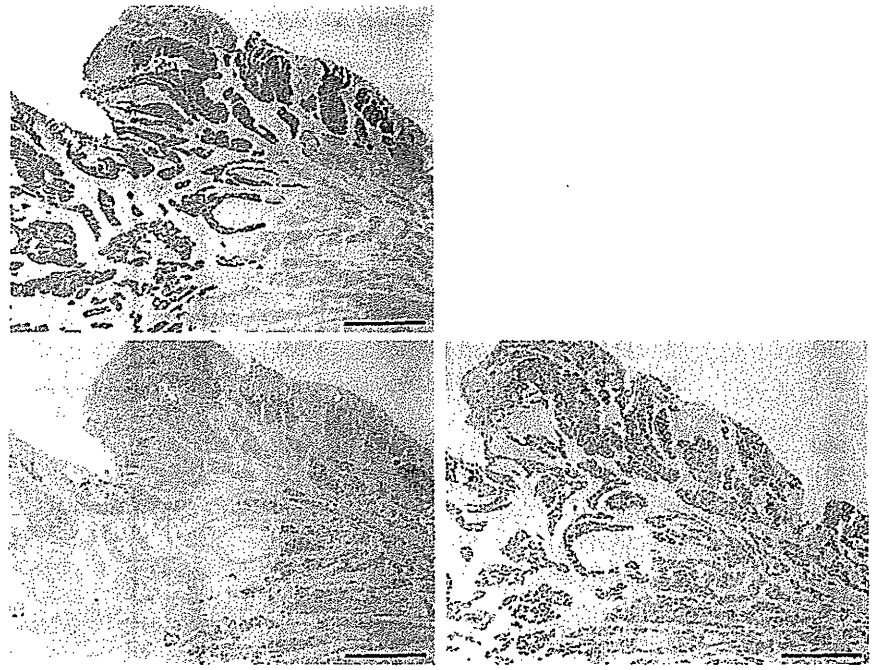

Fig. 6 The comparison between Aquaporin 5, p21, and cyclin D1 protein expressions in human ESCC tissues. Immunohistochemical staining patterns of AQP5 (*upper left*) and CCND1 (*lower right*) were similar and those of AQP5 and p21 (*lower left*) were contrasted, which supported results of microarray and verification studies as described in Supplementary Table 2 and Fig. 4. Magnification: ×40. *Bar* 1000 μm

crucial role in osmotic water transport [1, 2]. Recent studies have shown that AQPs are also found in various tumor tissues, where they perform unexpected functions. For example, AQPs have been associated with tumor progression. AQP5 is one of the 13 AQP subtypes characterized in humans [7, 8]. The molecular mechanism of AQP5 expression has been investigated in some studies [33–35]. Adamzik et al. revealed that a novel single nucleotide (−1364A/C) polymorphism in the AQP5 gene promoter altered AQP5 expression in HeLa cells [33]. Borok et al. [34] showed the common and tissue-specific regulations of AQP5 promoter activities using rat lung and salivary epithelial cells. Recent studies have also established its expression and role during tumor development in various cancers [13, 17–26]. However, the expression of AQP5 in human ESCC tissues and the pathophysiologic role of AQP5 expression in ESCC cells have not been previously reported.

The expression of AQP5 is correlated with cell proliferation in several cancers [18, 19, 23, 26]. For instance, Kang et al. [18] showed that downregulation of AQP5 reduced cell proliferation in colorectal cancer cell lines. In the present study, we also showed that downregulation of AQP5 inhibited cell proliferation in two ESCC cell lines (Fig. 2d). Furthermore, cell cycle analysis indicated that the knockdown of AQP5 with siRNA inhibited cell cycle progression from G_1 to S phase in these cell lines (Fig. 2c). These findings indicate that AQP5 expression may influence both cell proliferation and cell cycle progression.

Little is known about the role of AQP5 in cell survival. Chae et al. [26] reported that caspase9 activity increased and apoptosis was promoted in AQP5 siRNA-treated chronic myelogenous leukemia. However, the potential role of AQP5 in apoptosis in gastrointestinal cancers has gone unreported. The present study revealed that the knockdown of AQP5 in ESCC cells induced apoptosis and also enhanced staurosporine stimulus-induced apoptosis (Fig. 3).

Previous studies have reported on the molecular mechanism by which AQP5 may mediate tumor progression. Kang et al. [18] showed that, in colorectal cancer cell lines, the oncogenic property of AQP5 was mediated by the activation of Ras and the extracellular signal-regulated kinase (ERK), as well as the retinoblastoma protein (Rb) signaling pathway. They also showed that up-regulation of AQP5 increased the phosphorylation of ERK1/2 in colorectal cancer cells, while the up-regulation of AQP1 and AQP3 did not alter ERK1/2 phosphorylation. Zhang et al. [23] showed that the activity of the epidermal growth factor receptor (EGFR)/ERK/p38 mitogen-activated protein kinase (p38 MAPK) signaling pathway was enhanced by the overexpression of AQP5 in lung cancer cell lines. To determine how the down-regulation of AQP5 affects cell proliferation, we used a bioinformatics approach to analyze the genome-wide consequences of AQP5 knockdown. A microarray analysis showed that, among 2,132 genes with altered expression after AQP5 knockdown, 398 genes had cell proliferation related functions (Supplementary Table 2). "Cellular Growth and Proliferation" was the top-ranked signaling network associated with AQP5 knockdown-related genes (Supplementary Table 1). Among these 398 genes, we confirmed changes in the expression of

Table 2 Correlation between clinicopathological features and AQP5 expression

Variable	*n*	Grade of AQP5 expression		*p* value
		Negative (<3)	Positive (3≦)	
Total	68	27 (40 %)	41 (60 %)	
Gender				
Male	57	23 (85 %)	34 (83 %)	1.000
Female	11	4 (15 %)	7 (17 %)	
Age; years				
<65	39	15 (56 %)	24 (59 %)	1.000
65≦	29	12 (44 %)	17 (41 %)	
Size				
<50	48	24 (89 %)	24 (59 %)	0.008*
50≦	20	3 (11 %)	17 (41 %)	
Histological type				
Well/moderate	45	13 (48 %)	32 (78 %)	0.018*
Poor	23	14 (52 %)	9 (22 %)	
Preoperative chemotherapy				
Negative	64	25 (93 %)	39 (95 %)	1.000
Positive	4	2 (7 %)	2 (5 %)	
Lymphatic invasion				
Negative	32	15 (56 %)	17 (41 %)	0.323
Positive	36	12 (44 %)	24 (59 %)	
Venous invasion				
Negative	38	16 (59 %)	22 (54 %)	0.804
Positive	30	11 (41 %)	19 (46 %)	
Pathological depth of tumor				
1–2	43	20 (74 %)	23 (56 %)	0.199
3	25	7 (26 %)	18 (44 %)	
Pathological lymph node metastasis				
0	32	14 (52 %)	18 (44 %)	0.622
1-	36	13 (48 %)	23 (56 %)	
Pathological stage				
0–I	26	12 (44 %)	14 (34 %)	0.450
II–IV	42	15 (56 %)	27 (66 %)	
Postoperative recurrence (3-year)				
Negative	43	21 (78 %)	22 (54 %)	0.071
Positive	25	6 (22 %)	19 (46 %)	

* $p < 0.05$: Fisher's exact test

several cell proliferation related genes by knockdown of AQP5. We reconfirmed the results of microarray analysis by verification of 6 selected gene expressions using quantitative RT-PCR, and revealed that the expression levels of TP53INP1, CDKN1A ($p21^{CIP1/WAF1}$), and CCND1/cdk4, which are widely known as G_1/S checkpoint related genes [36, 37], were significantly altered upon down-regulation of AQP5 (Fig. 4). Further, we showed the immunohistochemical staining patterns of AQP5, p21, and CCND1 protein, which supported the results of microarray analysis

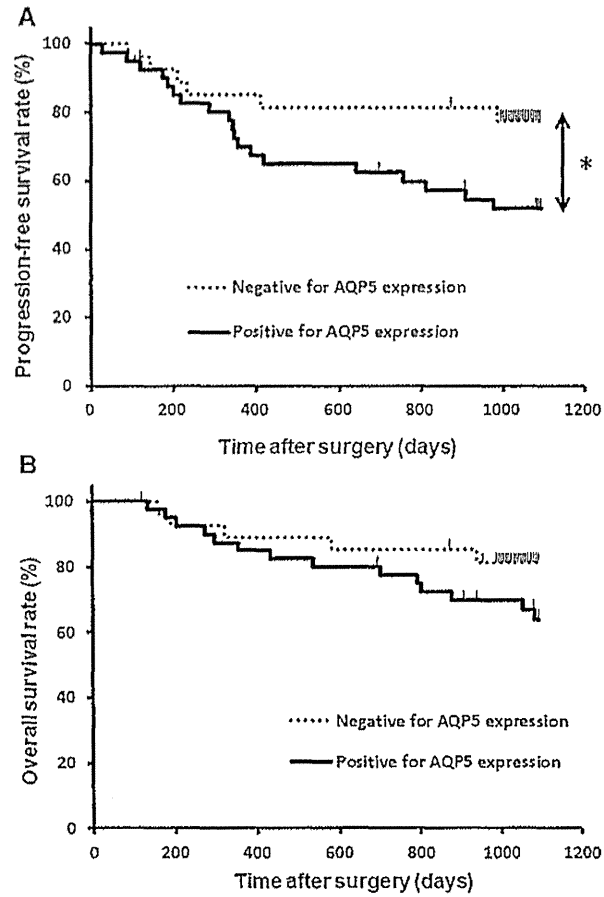

Fig. 7 The survival curves of 68 ESCC patients. **a** The 3-year progression-free survival rate of the AQP5 positive group was significantly poorer than that of the AQP5 negative group (log rank test, $p = 0.045$). **b** Although the 3-year overall survival rate of the AQP5 positive group was poorer than that of the AQP5 negative group, no significant difference was detected between two groups (log rank test, $p = 0.160$)

(Fig. 6). These results indicated the AQP5 expression level might influence the expression level of some important genes which were correlated with cell cycle progression.

To our knowledge, our immunohistochemical study is the first to investigate the clinicopathological and prognostic significance of AQP5 expression in human ESCC tissue samples. Kang et al. [18] examined 94 samples from colorectal cancer patients and showed that both age and metastasis status were significantly associated with AQP5 expression. Chae et al. [23] reported that among non-small cell lung cancer patients, only histological type was significantly associated with AQP5 expression, and the disease-free survival rate of AQP5-positive cases was significantly poorer than that of AQP5-negative cases. In the present study, we found that tumor size and the number of differentiated histological types in AQP5 positive patients were significantly larger than those of AQP5 negative patients (Table 2). Watanabe et al. showed that

Table 3 Univariate and multivariate analyses for prognostic factors associated with 3-year progression free survival

Variable	Number	3-year PFS	Univariate[a]		Multivariate[b]	
	$n = 68$	rate (%)	p value	HR	95 % CI	p value
Gender						
Male	57	61.1	0.572			
Female	11	68.6				
Age; years						
<65	39	55.1	0.122			
65≦	29	71.8				
Size						
<50	48	67.6	0.061			
50≦	20	50.0				
Histological type						
Well/moderate	45	63.3	0.633			
Poor	23	60.2				
Lymphatic invasion						
Negative	32	77.8	0.009*	2.056	0.851–5.513	0.111
Positive	36	48.4				
Venous invasion						
Negative	38	73.0	0.033*	1.655	0.727–3.933	0.231
Positive	30	48.3				
Pathological depth of tumor						
1–2	43	66.1	0.259			
3	25	56.0				
Pathological lymph node metastasis						
0	32	77.8	0.006*	2.583	1.106–6.736	0.028*
1-	36	48.0				
Grade of AQP5 staining						
Negative	27	77.8	0.045*	1.900	0.787–5.297	0.159
Positive	41	53.7				

PFS Progression free survival, *HR* hazard ratio, *CI* confidence interval

[a] Kaplan and Meier method, and the statistical significance was determined by log-rank test

[b] Multivariate analysis was performed using Cox proportional hazard model

overexpression of AQP5 induced cell differentiation in human gastric cancer cell lines [24]. These results suggest that AQP expression might be correlated with cell differentiation and morphological change in various cancers. Furthermore, our study also showed that the 3-year PFS rate of the AQP5 positive group was significantly poorer than that of the AQP5 negative group (Fig. 7a). These observations indicate that AQP5 expression is related to ESCC malignancy, including the risk of tumor recurrence, and it may be a useful indicator for selecting a postoperative treatment approach.

In summary, we have shown that AQP5 plays a role in the proliferation and survival of ESCC cells. Our microarray data also show that AQP5 affects the expression of other genes with functions related to cellular growth and proliferation. Immunohistochemistry revealed that the expression of AQP5 in human ESCC tissue is related to tumor size, histological type, and rate of recurrence in ESCC patients. Although further investigation of the molecular mechanism is necessary, our observations suggest that AQP5 may be a useful biomarker of tumor development and/or a novel therapeutic target for the future treatment of ESCC.

Acknowledgments This work was supported by Grants-in-Aid for Young Scientists (B) (22791295, 23791557, 24791440), a Grant-in-Aid for Scientific Research (C) (22591464, 24591957) from the Japan Society for the Promotion of Science.

Conflict of interest The authors declared that they have no conflict of interest.

References

1. King LS, Agre P. Pathophysiology of the aquaporin water channels. Annu Rev Physiol. 1996;58:619–48.
2. Verkman AS, van Hoek AN, Ma T, Frigeri A, Skach WR, Mitra A, et al. Water transport across mammalian cell membranes. Am J Physiol. 1996;270:C12–30.
3. Verkman AS. More than just water channels: unexpected cellular roles of aquaporins. J Cell Sci. 2005;118:3225–32.
4. Woo J, Lee J, Kim MS, Jang SJ, Sidransky D, Moon C. The effect of aquaporin 5 overexpression on the Ras signaling pathway. Biochem Biophys Res Commun. 2008;367:291–8.
5. Woo J, Lee J, Chae YK, Kim MS, Baek JH, Park JC, et al. Overexpression of AQP5, a putative oncogene, promotes cell growth and transformation. Cancer Lett. 2008;264:54–62.
6. Wang W, Zheng M. Role of cAMP-PKA/CREB pathway in regulation of AQP 5 production in rat nasal epithelium. Rhinology. 2011;49:464–9.
7. Agre P. The aquaporin water channels. Proc Am Thorac Soc. 2006;3:5–13.
8. Agre P, King LS, Yasui M, Guggino WB, Ottersen OP, Fujiyoshi Y, et al. Aquaporin water channels—from atomic structure to clinical medicine. J Physiol. 2002;542:3–16.
9. Krane CM, Melvin JE, Nguyen HV, Richardson L, Towne JE, Doetschman T, et al. Salivary acinar cells from aquaporin 5-deficient mice have decreased membrane water permeability and altered cell volume regulation. J Biol Chem. 2001;276:23413–20.
10. Karabasil MR, Hasegawa T, Azlina A, Purwanti N, Yao C, Akamatsu T, et al. Effects of naturally occurring G103D point mutation of AQP5 on its water permeability, trafficking and cellular localization in the submandibular gland of rats. Biol Cell. 2011;103:69–86.
11. Gresz V, Kwon TH, Gong H, Agre P, Steward MC, King LS, et al. Immunolocalization of AQP-5 in rat parotid and submandibular salivary glands after stimulation or inhibition of secretion in vivo. Am J Physiol Gastrointest Liver Physiol. 2004;287:G151–61.
12. Kreda SM, Gynn MC, Fenstermacher DA, Boucher RC, Gabriel SE. Expression and localization of epithelial aquaporins in the adult human lung. Am J Respir Cell Mol Biol. 2001;24:224–34.
13. Burghardt B, Elkaer ML, Kwon TH, Racz GZ, Varga G, Steward MC, et al. Distribution of aquaporin water channels AQP1 and AQP5 in the ductal system of the human pancreas. Gut. 2003;52:1008–16.
14. Shankardas J, Patil RV, Vishwanatha JK. Effect of down-regulation of aquaporins in human corneal endothelial and epithelial cell lines. Mol Vis. 2010;16:1538–48.
15. Dobbs LG, Gonzalez R, Matthay MA, Carter EP, Allen L, Verkman AS. Highly water-permeable type I alveolar epithelial cells confer high water permeability between the airspace and vasculature in rat lung. Proc Natl Acad Sci USA. 1998;95:2991–6.
16. Nielsen S, Frokiaer J, Marples D, Kwon TH, Agre P, Knepper MA. Aquaporins in the kidney: from molecules to medicine. Physiol Rev. 2002;82:205–44.
17. Moon C, Soria JC, Jang SJ, Lee J, Obaidul Hoque M, Sibony M, et al. Involvement of aquaporins in colorectal carcinogenesis. Oncogene. 2003;22:6699–703.
18. Kang SK, Chae YK, Woo J, Kim MS, Park JC, Lee J, et al. Role of human aquaporin 5 in colorectal carcinogenesis. Am J Pathol. 2008;173:518–25.
19. Jung HJ, Park JY, Jeon HS, Kwon TH. Aquaporin-5: a marker protein for proliferation and migration of human breast cancer cells. PLoS ONE. 2011;6:e28492.
20. Chae YK, Woo J, Kim MJ, Kang SK, Kim MS, Lee J, et al. Expression of aquaporin 5 (AQP5) promotes tumor invasion in human non small cell lung cancer. PLoS ONE. 2008;3:e2162.
21. Chen Z, Zhang Z, Gu Y, Bai C. Impaired migration and cell volume regulation in aquaporin 5-deficient SPC-A1 cells. Respir Physiol Neurobiol. 2011;176:110–7.
22. Machida Y, Ueda Y, Shimasaki M, Sato K, Sagawa M, Katsuda S, et al. Relationship of aquaporin 1, 3, and 5 expression in lung cancer cells to cellular differentiation, invasive growth, and metastasis potential. Hum Pathol. 2011;42:669–78.
23. Zhang Z, Chen Z, Song Y, Zhang P, Hu J, Bai C. Expression of aquaporin 5 increases proliferation and metastasis potential of lung cancer. J Pathol. 2010;221:210–20.
24. Watanabe T, Fujii T, Oya T, Horikawa N, Tabuchi Y, Takahashi Y, et al. Involvement of aquaporin-5 in differentiation of human gastric cancer cells. J Physiol Sci. 2009;59:113–22.
25. Yang JH, Shi YF, Cheng Q, Deng L. Expression and localization of aquaporin-5 in the epithelial ovarian tumors. Gynecol Oncol. 2006;100:294–9.
26. Chae YK, Kang SK, Kim MS, Woo J, Lee J, Chang S, et al. Human AQP5 plays a role in the progression of chronic myelogenous leukemia (CML). PLoS ONE. 2008;3:e2594.
27. Kusayama M, Wada K, Nagata M, Ishimoto S, Takahashi H, Yoneda M, et al. Critical role of aquaporin 3 on growth of human esophageal and oral squamous cell carcinoma. Cancer Sci. 2011;102:1128–36.
28. Lyons SA, Chung WJ, Weaver AK, Ogunrinu T, Sontheimer H. Autocrine glutamate signaling promotes glioma cell invasion. Cancer Res. 2007;67:9463–71.
29. Nishihira T, Hashimoto Y, Katayama M, Mori S, Kuroki T. Molecular and cellular features of esophageal cancer cells. J Cancer Res Clin Oncol. 1993;119:441–9.
30. Sobin LH, Gospodarowicz MK, Wittekind C, editors. TNM classification of malignant tumors. 7th ed. Hoboken: Wiley; 2009.
31. Taubert H, Heidenreich C, Holzhausen HJ, Schulz A, Bache M, Kappler M, et al. Expression of survivin detected by immunohistochemistry in the cytoplasm and in the nucleus is associated with prognosis of leiomyosarcoma and synovial sarcoma patients. BMC Cancer. 2010;10:65.
32. Wu SG, Chang YL, Lin JW, Wu CT, Chen HY, Tsai MF, et al. Including total EGFR staining in scoring improves EGFR mutations detection by mutation-specific antibodies and EGFR TKIs response prediction. PLoS ONE. 2011;6:e23303.
33. Adamzik M, Frey UH, Bitzer K, Jakob H, Baba HA, Schmieder RE, et al. A novel-1364A/C aquaporin 5 gene promoter polymorphism influences the responses to salt loading of the renin-angiotensin-aldosterone system and of blood pressure in young healthy men. Basic Res Cardiol. 2008;103:598–610.
34. Borok Z, Li X, Fernandes VF, Zhou B, Ann DK, Crandall ED. Differential regulation of rat aquaporin-5 promoter/enhancer activities in lung and salivary epithelial cells. J Biol Chem. 2000;275:26507–14.
35. Zhou B, Francis TA, Yang H, Tseng W, Zhong Q, Frenkel B, et al. GATA-6 mediates transcriptional activation of aquaporin-5 through interactions with Sp1. Am J Physiol Cell Physiol. 2008;295:C1141–50.
36. Carnero A, Hannon GJ. The INK4 family of CDK inhibitors. Curr Top Microbiol Immunol. 1998;227:43–55.
37. Lukas J, Bartkova J, Bartek J. Convergence of mitogenic signalling cascades from diverse classes of receptors at the cyclin D-cyclin-dependent kinase-pRb-controlled G1 checkpoint. Mol Cell Biol. 1996;16:6917–25.

Middle and lower esophagectomy preceded by hand-assisted laparoscopic transhiatal approach for distal esophageal cancer

ATSUSHI SHIOZAKI, HITOSHI FUJIWARA, HIROTAKA KONISHI, RYO MORIMURA, SHUHEI KOMATSU, YASUTOSHI MURAYAMA, YOSHIAKI KURIU, HISASHI IKOMA, TAKESHI KUBOTA, MASAYOSHI NAKANISHI, DAISUKE ICHIKAWA, KAZUMA OKAMOTO, CHOUHEI SAKAKURA and EIGO OTSUJI

Division of Digestive Surgery, Department of Surgery, Kyoto Prefectural University of Medicine, Kyoto 602-8566, Japan

Received April 26, 2013; Accepted October 10, 2013

DOI: 10.3892/mco.2013.201

Abstract. Respiratory morbidity is the most frequent complication following an esophagectomy. This study was designed to determine the efficacy of middle and lower esophagectomies preceded by the hand-assisted laparoscopic transhiatal approach (LTHA) regarding the perioperative outcomes of distal esophageal cancer. The esophageal hiatus was opened and carbon dioxide was introduced into the mediastinum. Dissection of the distal esophagus was performed up to the level of the tracheal bifurcation. En bloc dissection of the posterior mediastinal lymph nodes was performed using the LTHA. Subsequently, a small thoracotomy (10 cm) was performed to divide the thoracic esophagus and allow middle mediastinal lymphadenectomy. Finally, reconstruction via the posterior mediastinal route with a gastric tube and anastomosis in the thoracic cavity were performed using a circular stapler. The treatment outcomes of 10 patients who underwent LTHA-preceded middle and lower esophagectomy were compared to those of 11 patients treated without prior LTHA (thoracotomy, 20 cm). The total operative time, the duration of one-lung ventilation and total operative blood loss were significantly decreased in the LTHA group. The number of resected lymph nodes did not differ significantly between the two groups. Postoperative respiratory complications occurred in 10.0% of patients treated with, and 36.3% of those treated without LTHA. The extubation time following surgery, the duration of thoracic drainage and postoperative hospital stay were significantly decreased by this method. In conclusion, middle and lower esophagectomies preceded by LTHA provides a good surgical view of the posterior mediastinum, markedly shortens the duration of one-lung ventilation and improves the perioperative outcome.

Correspondence to: Dr Atsushi Shiozaki, Division of Digestive Surgery, Department of Surgery, Kyoto Prefectural University of Medicine, 465 Kajii-cho, Kamigyo-ku, Kyoto 602-8566, Japan
E-mail: shiozaki@koto.kpu-m.ac.jp

Key words: laparoscopic transhiatal approach, distal esophageal cancer

Introduction

Esophagectomies is associated with significant morbidity and mortality, although recent advances in surgical and postoperative management techniques have improved the treatment outcome (1). Respiratory morbidity, in particular, remains the most common serious complication following esophagectomy and a number of studies demonstrated a respiratory complication rate of ~20% (2-5). Since the duration of one-lung ventilation is known to affect postoperative immune reactions and cause respiratory complications, it is crucial to reduce the intrathoracic operative time (6,7).

We first performed an esophagectomy preceded by the laparoscopic transhiatal approach (LTHA) for patients with esophageal cancer in 2009 (8-10). With this method, carbon dioxide is introduced into the mediastinum from the abdominal side of the diaphragm and middle and lower mediastinal operations may be performed via a transhiatal approach. The main advantages of this method are that the thoracic procedures performed via right thoracotomy may be simplified and the duration of one-lung ventilation may be shortened. In addition, a good surgical view of the lower mediastinum is obtained and the quality of the mediastinal surgery may be improved. By December, 2012, a total of 121 patients with esophageal tumors had undergone LTHA during a variety of esophageal surgical procedures, including subtotal esophagectomy, middle and lower esophagectomy and tumor resection (8-11).

In our previous study, we demonstrated the efficacy of LTHA preceding subtotal esophagectomy with gastric tube reconstruction via a retrosternal route, with regard to perioperative outcomes (8). In this study, we aimed to analyze the perioperative treatment outcomes of patients with distal esophageal cancer who underwent middle and lower esophagectomy preceded by hand-assisted LTHA and gastric tube reconstruction via the posterior mediastinal route (anastomosis in the thoracic cavity). Our results revealed that our method markedly shortened the duration of one-lung ventilation and decreased intraoperative blood loss. Furthermore, this method improved postoperative care by decreasing the extubation time following surgery, the duration of thoracic drainage and the length of the postoperative hospital stay.

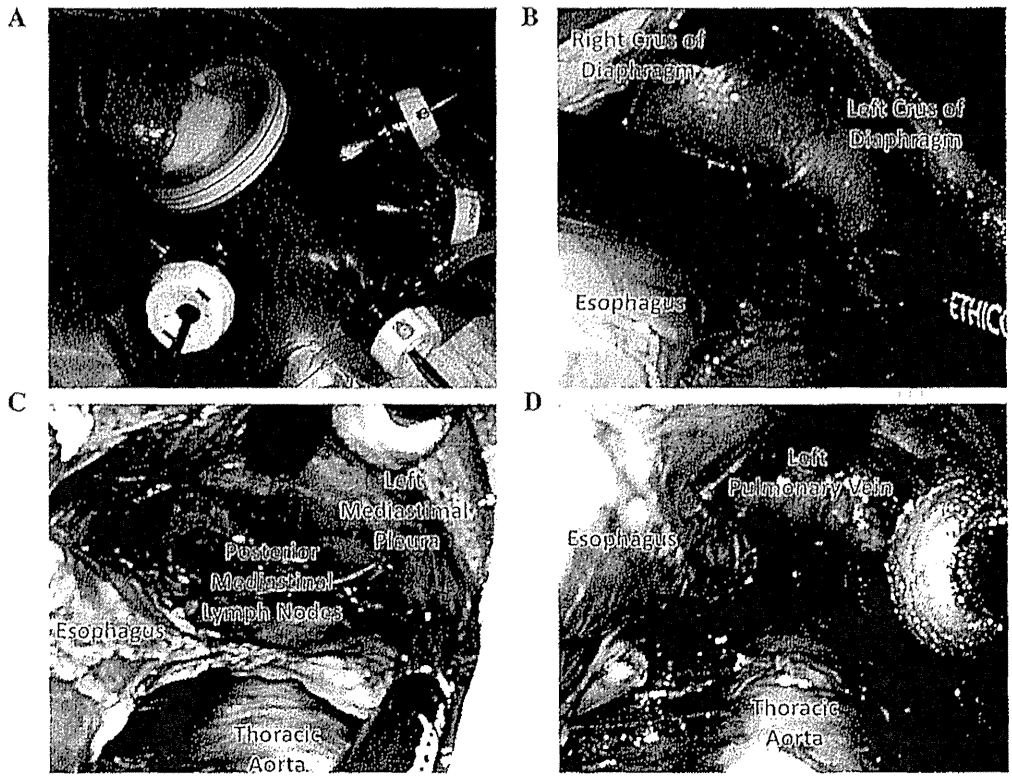

Figure 1. (A) Intraoperative view of the trocars and incision locations on the abdomen. A lap disc (regular) was placed in the upper abdomen. Three 12-mm ports were inserted, one in each flank and one in the left hypochondrium; one 5-mm port for the videoscope was inserted in the lower abdomen. (B) The esophageal hiatus was divided and carbon dioxide was introduced into the mediastinum. Dissection of the anterior sides of the posterior mediastinal lymph nodes was performed with the EnSeal device. (C) The anterior and posterior sides of the posterior mediastinal lymph nodes were resected: while lifting up these lymph nodes like a membrane, they were cut along the borderline of the left mediastinal pleura. (D) The posterior mediastinal lymph nodes (thoracic paraaortic and left pulmonary ligament lymph nodes) were dissected en bloc.

Patients and methods

Surgical procedure. An abdominal operation was performed using hand-assisted laparoscopic surgery (HALS). Subsequently, middle and lower mediastinal operations were performed using LTHA. The patients were placed in a supine position on the operating table. An upper abdominal incision (70 mm) was performed and a Lap Disc (regular) (Ethicon Endo-Surgery, Cincinnati, OH, USA) was placed (Fig. 1A). Three 12-mm ports were inserted, one in each flank and one in the left hypochondrium; one 5-mm port for the flexible laparoscope was inserted into the lower abdomen (Fig. 1A). The operator stood on the right side of the patient and inserted the Lap Disc with their left hand. The 12-mm port in the right flank was mainly used for the surgery. The assistant stood on the left side of the patient and the ports in the left abdomen were used to provide assistance. The scopist stood near the patient's groin. Carbon dioxide was introduced into the intra-abdominal space and the pneumoperitoneum pressure was controlled at 10 mmHg (8-11).

The operator lifted up the stomach with their left hand and the greater omentum, left gastroepiploic vessels and gastrosplenic ligament were divided using the EnSeal device (Ethicon Endo-Surgery). Subsequently, the esophageal hiatus was opened and carbon dioxide was introduced into the mediastinum. The assistant inserted an Endo Retract (Autosuture Norwalk, CT, USA) and a blunt tip dissector through the ports on the left side and the working space in the mediastinum was secured with these two devices and 10 mmHg of pneumomediastinum pressure. Dissection of the anterior and left side of the distal esophagus up to the level of the tracheal bifurcation was performed with the EnSeal device and the blunt tip dissector. Using this approach, dissection of the anterior sides of the posterior mediastinal lymph nodes was easily performed (Fig. 1B) (9).

Subsequently, the adventitia of the thoracic aorta was exposed at the level of the crura of the diaphragm, followed by dissection of the anterior side of the thoracic aorta to the cranial side. The roots of the proper esophageal arteries were confirmed and divided using the EnSeal device. Following these procedures, the anterior and posterior sides of the posterior mediastinal lymph nodes, including the thoracic paraaortic and left pulmonary ligament lymph nodes, were dissected. While lifting these lymph nodes like a membrane, they were cut along the borderline of the left mediastinal pleura (Fig. 1C). In this manner, the posterior mediastinal lymph nodes were dissected en bloc (Fig. 1D) (8,9).

Following the dissection of posterior mediastinal lymph nodes, the adventitia of the thoracic aorta and the crura of the diaphragm were exposed. Therefore, the appropriate layer for the dissection of the celiac lymph nodes was clearly identified and the dissection of the posterior mediastinal lymph nodes was extended towards the caudal side from the crura of the diaphragm to the celiac artery (Fig. 2A). The lymph nodes in the esophageal hiatus of the diaphragm, the infradiaphragmatic lymph nodes and the lymph nodes along the celiac artery were dissected en bloc from the left side approach. Subsequently, the left gastric vessels were exposed from the